Thin film flow over an unsteady stretching sheet with thermocapillarity in presence of magnetic field

Kalidas Das*

Dept.of Mathematics, A.B.N.Seal College, Cooch Behar, W.B., Pin-736101, India

email:kd_kgec@rediffmail.com

Nilangshu Acharya

Dept. of Mathematics, Narula Institute of Technology, Kolkata-700109, W.B., India

email:nilangshu.math@gmail.com

Prabir Kumar Kundu

Dept. of Mathematics, Jadavpur University, Kolkata 700032, W.B., India

e.mail: kunduprabir@yahoo.co.in

Abstract: *An analysis is carried out to study the effects of thermocapillarity on thin film flow over an unsteady stretching sheet in presence of uniform transverse magnetic field and internal heat source/sink. Using a similarity transformation the governing time dependent boundary layer equations are reduced to a set of coupled ordinary differential equations and then solved numerically for some representative values of non-dimensional parameters using Nachtsheim and Swigert shooting iteration technique together with Runge-Kutta sixth-order integration scheme. It is observed that the thermocapillary action reduces the rate of heat transfer at the surface while dealing with conducting fluid in presence of magnetic field.*

Key Words: *Thermocapillarity; Thin film; Magnetic field; Internal heat source/sink*

1. Introduction :

The fluid flow over a stretching sheet is relevant to several important engineering applications in the field of aerodynamics, metallurgy and chemical engineering processes such as metal and polymer extrusion, drawing of plastic sheets etc. The steady two dimensional boundary layer flow of Newtonian fluid over a stretching surface has been studied by Crane [1]. After this pioneering work the flow field over a stretching surface has drawn considerable attention and a good amount of literature has been generated on this problem [2-7].

The analysis of laminar flow of a thin liquid film over a stretching sheet has attracted the attention of growing number of researchers because of its various applications in different branches of engineering. The concept of flow and heat transfer characteristics within a thin liquid film is very important for better understanding the coating processes. Other applications can be found in food stuff processing, transpiration cooling and so on. Wang [8] first studied the hydrodynamics of thin liquid film flow over a stretching sheet and solved the resulting equations by employing a multiple shooting method (see [9]). Andersson et al. [10] discussed the problem by considering the effect of heat transfer. To reinvestigate thin film flow over a stretching sheet, Wang [11] used homotopy analysis method . Aziz et al. [12] generalized the work of Wang [8] by including internal heat generation. Lately, the work of Wang [8] has been extended by several researchers ([13-16]) under different boundary conditions.

The term "thermocapillarity" refers to phenomena that arise as a consequence of the variation of interfacial surface-tension at a fluid interface caused by temperature differences. These surface-tension gradients generate an interfacial flow that, through viscous drag, either oppose or support the shear driven motion due to stretching sheet. The effect of the thermocapillarity on the heat transfer in a liquid film on a stretching surface was studied by Dandapat et al. [17]. In another study Dandapat et al. [18] investigated the influence of the thermocapillarity on flow and heat transfer in a laminar liquid film when the fluid properties are variable.

Many researchers have been conducted to study the effects of electrically conducting fluids on the thin film flow and heat transfer in presence of magnetic field. Abel et al. [19] discussed the influence of magnetic field on heat transfer in a liquid film over an unsteady stretching surface. Noor et al. [20] studied MHD flow and heat transfer in a thin liquid film on an unsteady stretching. The effect of thermocapillarity and magnetic field in a thin film flow on an unsteady elastic stretching sheet was considered by Noor and Hashim [21]. Later, thin film flow over a heated nonlinear stretching sheet in presence of uniform transverse magnetic field was studied by Dandapt and Singh [22]. *Das and* Zheng [23] investigated the influence of melting heat transfer on the stagnation point flow of an electrically conducting MHD Jeffrey fluid past a semi-infinite stretching sheet in the presence of viscous dissipation and Joule heating. Das [24] studied the hydromagnetic incompressible electrically conducting fluid flow over a permeable stretching surface with slip boundary conditions. MHD mixed convective heat and mass transfer flow of an electrically conducting second grade fluid past a semi-infinite stretching sheet in the presence of thermal diffusion was studied by Das [25]. Das et al. [26] discussed thermophoretic effect on hydromagnetic slip flow over a permeable flat plate in the presence of non-uniform heat source/sink. The aim of the present investigation is to extend the model in Aziz et al. [12] by including thermocapillary effect in presence of external transverse magnetic field and internal heat source/sink.

2. Mathematical Modelling

Consider a conducting incompressible Newtonian liquid film over a heated elastic sheet that emerges from a narrow slit at the origin of the Cartesian coordinate system for investigations as shown schematically in Fig. 1. A thin film of uniform thickness h(t) lies on the horizontal stretching sheet. The liquid motion within the film is caused solely by stretching sheet. The continuous sheet is parallel to x-axis and moves in its own plane with velocity

$$U = \frac{bx}{1-\alpha t} \tag{1}$$

where α and b are positive constants with dimension per time. The elastic sheet's temperature T_s is assumed to vary with the distance x from the slit as

$$T_s\left(x,t\right) = T_0 - T_{ref}\left[\frac{bx^2}{2\nu}\right]\left(1-\alpha t\right)^{-3/2} \tag{2}$$

where T_0 is the temperature of the liquid at the slit, T_{ref} is the constant reference temperature such that $0 \le T_{ref} \le T_0$ for all $t<1/\alpha$. A transverse magnetic field $B=B_0/(1-\alpha t)^{1/2}$ is applied to the thin liquid film. The liquid properties are taken to be constant, except that the surface tension that varies linearly with temperature as [21]

$$\sigma = \sigma_0\left[1-\delta\left(T-T_0\right)\right] \tag{3}$$

In general σ decreases with temperature for most liquids so that $\delta > 0$. It is assumed that the pressure in the surrounding gas phase is uniform and the gravity gives rise to a hydrostatic variation in the liquid film.

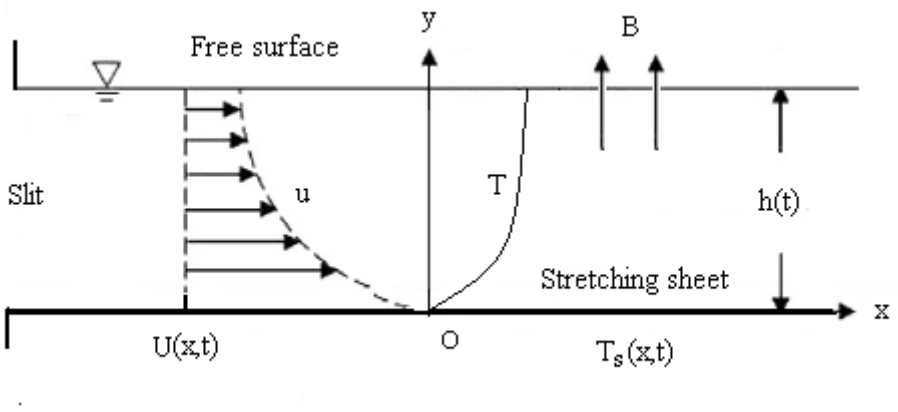

Figure 1. Physical model and coordinate system

Under these assumptions, the motion of liquid film due to stretching is governed by

$$\frac{\partial u}{\partial x}+\frac{\partial v}{\partial y}=0 \tag{4}$$

$$\frac{\partial u}{\partial t}+u\frac{\partial u}{\partial x}+v\frac{\partial u}{\partial y}=\nu\frac{\partial^2 u}{\partial y^2}-\frac{\sigma^* B^2}{\rho}u \tag{5}$$

$$\rho C_p\left(\frac{\partial T}{\partial t}+u\frac{\partial T}{\partial x}+v\frac{\partial T}{\partial y}\right)=\kappa\frac{\partial^2 T}{\partial y^2}+Q \tag{6}$$

where u and v are the velocity components of liquid in x- and y- directions, T is the temperature, ν is the kinematic viscosity, μ is the dynamic viscosity, ρ is the density, C_p is the specific heat at constant pressure, κ is the thermal conductivity, σ* is the electrical conductivity and σ is the surface tension. The term Q is the heat generation (>0) or absorption (<0) per unit volume which is modelled as [12]

$$Q=\frac{\kappa U}{x\nu}B^*\left(T-T_0\right) \tag{7}$$

where B^* is the temperature-dependent heat generation/absorption and is positive in the case of the elastic sheets' generation of heat and negative in the case of the sheet's absorption of heat from the fluid flow. To justify the boundary layer approximation, it is assumed that the length scale in the primary flow direction is sufficiently large than the length scale in the cross stream direction. The representative measure of the film thickness is chosen to be $(\upsilon/b)^{1/2}$ so that the scale ratio is large enough i.e., $x/(\upsilon/b)^{1/2}>>1$. This choice of scale enables us to apply the boundary layer approximations.

The boundary conditions on the stretching sheet are no slip, no penetration and imposed sheet temperature distribution and they are represented respectively as

$$\left.\begin{aligned} &u=U,\ v=0,\ T=T_S \text{ at } y=0,\\ &\mu\frac{\partial u}{\partial y}=\frac{\partial \sigma}{\partial x},\ \frac{\partial T}{\partial y}=0,\ v=\frac{dh}{dt} \text{ at } y=h \end{aligned}\right\} \tag{8}$$

The following similarity transformations are introduced

$$\psi=\beta x\left[\frac{\nu b}{1-\alpha t}\right]^{1/2}f(\eta),\ T=T_0-T_{ref}\left[\frac{bx^2}{2\nu\left(1-\alpha t\right)^{3/2}}\right]\theta(\eta),\ \eta=\frac{1}{\beta}\left[\frac{b}{\nu\left(1-\alpha t\right)}\right]^{1/2}y \tag{9}$$

where β is the dimensionless film thickness, defined as [8, 11]

$$\beta = \left[\frac{b}{\nu(1-\alpha t)}\right]^{1/2} h \tag{10}$$

Also, ψ (x, y) is the stream function which automatically assures mass conversation (4). The velocity components are readily obtained as

$$u = \frac{\partial \psi}{\partial y} = \frac{bx}{1-\alpha t} f'(\eta), \quad v = -\frac{\partial \psi}{\partial x} = -\left(\frac{\nu b}{1-\alpha t}\right)^{1/2} \beta f(\eta) \tag{11}$$

where prime denotes differentiation with respect to η. Thus the mathematical problem defined through Eqs. (4)- (9) are transformed to the following non-linear boundary value problem on the finite range of 0-1:

$$f''' + \beta^2 \left[ff'' - \frac{1}{2} S\eta f'' - f'^2 - \left(S + Ha^2\right) f' \right] = 0 \tag{12}$$

$$\theta'' + \beta^2 \left[\Pr\left(f\theta' - 2f'\theta - \frac{1}{2} S\eta\theta' - \frac{3}{2} S\theta \right) + B^* \theta \right] = 0, \tag{13}$$

subject to

$$\left.\begin{aligned} &f(0) = 0,\ f'(0) = 1,\ \theta(0)=1, \\ &f(1) = \frac{1}{2} S,\ f''(1) = M\theta(1),\ \theta'(1) = 0 \end{aligned}\right\} \tag{14}$$

where $S = \frac{\alpha}{b}$ is the dimensionless measure of unsteadiness, $Ha = B_0 \sqrt{\frac{\sigma^*}{\rho b}}$ is the Hartmann number, $M = \frac{\delta \sigma_0 T_{ref} \beta}{\mu \sqrt{b\nu}}$ is the thermocapillarity number, $\Pr = \frac{\rho C_p \nu}{\kappa}$ is the Prandtl number.

The parameters of engineering interest in heat transfer problems are the Skin friction coefficient C_f and the Nusselt number Nu. These parameters characterize surface drag and heat transfer rate and are defined respectively, as

$$C_{fr} = C_f \, \mathrm{Re}_x^{1/2} = \frac{2}{\beta} f''(0) \tag{15}$$

$$Nur = Nu\,\mathrm{Re}_x^{-3/2} = \frac{1}{2\beta}\theta'(0)\left(1-\alpha t\right)^{-1/2} \tag{16}$$

where C_{fr} is the reduced skin friction coefficient, Nur is the reduced Nusselt number and $Re_x=Ux/\nu$ is the local Reynolds number.

3. Method of Solution

The coupled non-linear ordinary differential equations (10)-(13) with the boundary conditions (14) form a boundary value problem (BVP). First we convert these higher order equations to first order equation of higher dimension as follows:

$$\left.\begin{aligned} f_0' &= f_1 \\ f_1' &= f_2 \\ f_2' &= \beta^2\left[f_1^{\,2} + \left(S + Ha^2\right) f_1 + \frac{1}{2} S\eta f_2 - f_0 f_2 \right] \\ \theta_0' &= \theta_1 \\ \theta_1' &= \beta^2\left[\mathrm{Pr}\left(2 f_1\theta_0 + \frac{1}{2} S\eta\theta_1 + \frac{3}{2} S\theta_0 - f_0\theta_1 \right) - B^*\theta_0 \right] \end{aligned}\right\} \tag{17}$$

with the boundary conditions

$$\left.\begin{aligned} & f_0(0) = 0,\ f_1(0) = 1,\ \theta_0(0) = 0 \\ & f_0(1) = \frac{1}{2} S,\ f_2(1) = M\theta_0(1),\ \theta_1(1) = 0 \end{aligned}\right\} \tag{18}$$

Here $f_0(\eta) = f(\eta),\ \ \theta_0(\eta) = \theta(\eta)$. The above set of equations (17) under the boundary conditions (18) is solved numerically by applying shooting iteration technique together with Runge-Kutta sixth order integration scheme. For that we require a value $f_2(0)$ and $\theta_1(0)$ but no such values are given in the boundary. The suitable guess values for $f_2(0)$ and $\theta_1(0)$ are chosen and then integration is carried out. A step size of $\Delta\eta = 0.001$ is selected for computation purpose. In general the numerical solutions are not satisfying the auxiliary terminal condition $f_0(1) = \frac{1}{2} S$ for a given value of S. Thus the estimated value of S is therefore systematically adjusted until the auxiliary terminal condition is satisfied within a tolerance limit of 10^{-6}.

3.1. Verification of the Code

In order to ascertain the accuracy of our numerical results, the present study (in absence of thermocapillarity number and Hartmann number) is compared with those of Aziz et al. [12] and Wang [11]. The values of skin friction coefficient -f "(0), free surface temperature θ (1) and heat transfer rate -θ '(0) have been calculated for various values of S and Pr and are presented in tables 1 and 2. From these tables, one can easily infer that our results are in excellent agreement with those of previously published work. Thus the use of the present numerical code for current model is justified.

Table 1. Skin friction coefficient -f ´´ (0) when Ha=M=0, Pr =1

	Present Work		Aziz et al.[12]		Wang[11]	
S	β	$-f''(0)$	β	$-f''(0)$	β	$-f''(0)$
0.8	2.151994	2.6809430214	2.151994	2.680943	2.15199	2.68094
1.0	1.543626	1.9723777720	1.543616	1.972384	1.54362	1.97238
1.2	1.127780	1.4444265502	1.127780	1.442625	1.127780	1.442631
1.4	0.821055	1.0127845562	0.821032	1.012784	0.821032	1.012784
1.6	0.576173	0.6423988882	0.576173	0.642397	0.567173	0.642397

Table 2. Free surface temperature θ(1) and the rate of heat transfer -θ´(0) when Ha=M=0, S =0.8, B*=0, β=2.15199

	Present Work		Aziz et al.[12]		Wang[11]	
Pr	θ(1)	$-\theta'(0)$	θ(1)	$-\theta'(0)$	θ(1)	$-\theta'(0)$
1	0.09788441554	3.5959828553	0.097956	3.591125	0.097884	3.595970
2	0.02508311115	5.0741869571	0.025083	5.074186	0.024941	50244150
3	0.00854442213	5.9265472123	0.008545	5.926547	0.008785	6.514440

4. Results and Discussions

To provide a physical insight into the problem, comprehensive numerical computations are carried out using the method described in the previous section for various values of Hartmann number Ha, thermocapillarity number M, temperature dependent heat generation/absorption parameter B* and unsteadiness parameter S. In the simulation the default values of the parameters are considered as Pr=1.0, Ha=0.5, M=1.0, S =0.8, B*=0.05 and β =0.5 unless otherwise specified. The numerical results are presented in Figs.2-10.

4.1. Computational results for velocity profiles

The influence of Hartmann number Ha on the velocity distribution in thin film flow over an unsteady stretching sheet is presented in fig-2. It is observed from Fig. 2 that the fluid velocity decreases with increase in the values of Ha within the region η <0.7(not precisely determined) but outside this region these profiles overlap and increases with increase of Ha. Thus, the flow velocity leads to a decrease due to application of the transverse magnetic field near the stretching surface. The reason

behind this phenomenon is that, a resistive force similar to a drag force is produced which is known as the Lorentz force. It is to be noted here that the external transverse magnetic field produces an outward flow along the free surface. The effect of unsteadiness parameter S on velocity profiles in the presence of other involved parameters is presented in Fig.3. The velocity of flow increases significantly with an increment in S.

4.2. Computational results for temperature profiles

The effect of the Hartmann number Ha on the temperature distribution is shown in Fig. 4 in presence (i.e. S=0.8) and absence (i.e. S=0) of unsteadiness parameter S. One may observed that the increase in the values of Ha results an increase in fluid temperature in the free surface region. It is worth mentioning that the effect of Ha is prominent for steady case i.e. for S=0. The influence of the thermocapillarity number M over temperature field is presented in Fig.5 for both steady and unsteady case. It can be concluded that increase in the value of M will cause a decline in temperature. It may also be noted that the thermocapillarity does not affect the temperature near the stretching surface. The impact of unsteadiness parameter S on temperature profiles are illustrated in Fig.6. One can observe from the figure that the temperature of thin film decreases with S. The temperature profile due to the variation of the temperature dependent heat generation/absorption parameter B^* is depicted in Fig.7. It is evident from the figure that the temperature increases with increase in the value of B^*. Thus, the temperature dependent heat generation/absorption parameter B^* can speed up the cooling/heating of the thin film flow.

4.3. Computational results for skin friction and Nusselt number

The variation of the reduced skin friction coefficient C_{fr} versus Ha is plotted in Fig. 8 for different values of M while other parameters are kept fixed. It is evident from this plot that the increasing the values of M decrease the skin friction coefficient. On the other hand, C_{fr} increases monotonically when Ha is increased from 0 to 1.5 for fixed values of M. The quantity Nur that highlights surface heat transfer is shown as a function of Ha in Fig. 9 for different values of the thermocapillarity number M. Thus, the magnetic field has a considerable impact in controlling the heat transfer in the thin film flow. Fig. 10 depicts the variation of Nusselt number Nur with respect to the unsteadiness parameter S for different values of the temperature dependent heat generation/absorption parameter B*. From the figure, for any given value of B* one may observe that the rate of heat transfer increases with increasing the values of unsteadiness parameter S. Further, increasing the values of B* causes a fall in the rate of heat transfer at the sheet.

5. Conclusions

A theoretical study of the boundary layer behaviour in a thin film flow over an unsteady stretching sheet is carried out including the effects of uniform transverse magnetic field and internal heat source/sink. The governing equations are solved numerically by using Nachtsheim and Swigert shooting iteration technique together with Runge-Kutta sixth order integration scheme. A parametric study is performed to explore the effects of various governing parameters on fluid flow and heat transfer characteristics. Based on the present investigation the following inferences can be drawn:

- The transverse magnetic field suppresses the velocity field which in turn causes the enhancement of the temperature field in thin film flow.

- The flow temperature consistently cools down when the thermocapillarity number increases in presence of magnetic field.

- The skin friction coefficient decreases with increase in the thermocapillarity number whereas the effect is opposite for Hartmann number.

- Moreover, the rate of heat transfer at the stretching surface decreases with increasing the values of Hartmann number, thermocapillarity number and temperature dependent heat generation/absorption parameter.

Acknowledgements. The authors are very thankful to the reviewers and the Editor-in-chief for their constructive comments which have improved significantly the quality of the paper.

References

1. Crane, L.J. , Flow past a stretching plate. *Zeitschrift für angewandte Mathematik und Physik*

21 (1970), 4, pp. 645-647

2. Schlichting, H., Boundary-layer theory. New York: McGraw-Hill. 1955.

3. Afzal, N., Varshney, I.S., The cooling of a low heat resistance stretching sheet moving through a fluid. *Warme- und Stoffubertragung*. 14 (1980), 2, pp. 289-293

4. Ali, M.E., Heat transfer characteristics of a continuous stretching surface. *Warme- und Stoffubertragung*. 29(1994), 4, pp. 227-234

5. Ishak, A., et al., Boundary layer flow and heat transfer over an unsteady stretching vertical surface. *Meccanica*. 44 (2009), 4, pp. 369-375

6. Mabood, F., Khan, W.A., Ismail, A.I.Md., MHD stagnation point flow and heat transfer impinging on stretching sheet with chemical reaction and transpiration. Chemical Engineering Journal 273 (2015), 3, pp. 430–437.

7. Mabood, F., Khan, W.A., Ismail, A.I.Md., MHD boundary layer flow and heat transfer of nanofluids over a nonlinear stretching sheet: A numerical Study. Journal of Magnetism and Magnetic Materials 374 (2015), 11, pp. 569–576.

8. Wang, C.Y., Liquid film on an unsteady stretching surface. *Quarterly of Applied Mathematics*. 48 (1990), 3, pp. 601–610

9. Roberts, S.M. , Shipman, J.S., Two Point Boundary Value Problems: Shooting Methods. New York: Elsevier. 1972.

10. Andersson, H.I., et al., Heat transfer in a liquid film on an unsteady stretching surface. *International Journal of Heat and Mass Transfer*. 43 (2000), 1, pp. 69–74

11. Wang, C., Analytic solutions for a liquid film on an unsteady stretching surface. *Heat and Mass Transf*er. 42 (2006), 8, pp. 759-766

12. Aziz, R.C., et al., Thin film flow and heat transfer on an unsteady stretching sheet with internal heating. *Meccanica*. 46 (2011), 2, pp. 349-357

13. Liu, I.C., Andersson, H.I., Heat transfer in a liquid film on an unsteady stretching sheet. *International Journal of Thermal Sciences*, 47 (2008), 6, pp. 766–772

14. Usha, R., Sridharan, R., On the motion of a liquid film on an unsteady stretching surface. *ASME Fluids Engineering*. 150 (1993), 1, pp. 43-48

15. Chen, C.H., Heat transfer in a power-law fluid film over an unsteady stretching sheet. *Heat and Mass Transfer*. 39 (2003), 8-9, pp. 791–796

16. Chen, C.H., Marangoni effects on forced convection of power law liquids in a thin film over an unsteady stretching sheet. *Physics Letters A.* 370 (2007), 1, pp.51-57

17. Dandapat, B.S., et al., Thermocapillarity in a liquid film on an unsteady stretching surface. *International Journal of Heat and Mass Transfer* 46 (2003), 16, pp. 3009-3015

18. Dandapat, B.S., et al., The effects of variable fluid properties and thermocapillarity on the flow of a thin film on an unsteady stretching sheet. *International Journal of Heat and Mass Transfer*. 50 (2007), 5-6, pp. 991-996

19. Abel, M.S., et al., Heat transfer in a liquid film over an unsteady stretching surface with viscous dissipation in presence of external magnetic field. *Applied Mathematical Modelling.* 33 (2009), 8, pp. 3430-3441

20. Noor, N.F.M., et al., MHD flow and heat transfer in a thin liquid film on an unsteady stretching by the homotopy analysis method. *International Journal for Numerical Methods in Fluids.* 63 (2010), 3, pp. 357–373

21. Noor, N.F.M., Hashim, I., Thermocapillarity and magnetic field effects in a thin liquid on an unsteady stretching surface. *International Journal of Heat and Mass Transfer*. 53 (2010), 9-10, pp. 2044-2051

22. Dandapat, B.S., Singh, S.K., Thin film flow over a heated nonlinear stretching sheet in presence of uniform transverse magnetic field. *International Communications in Heat and mass Transfer*. 38 (2011), 3, pp. 324-328

23. *Das K*, Zheng L., Melting effects on the stagnation point flow of a Jeffrey fluid in the presence of magnetic field, *Heat Transfer Research*. 44 (2013), 6, pp. 493–506

24. Das K., A mathematical model on magnetohydrodynamic slip flow and heat transfer over a

non-linear stretching sheet, *Thermal Science*, 17 (2013), S2, pp. S475-S488

25. Das K., Influence of chemical reaction and viscous dissipation on MHD mixed convection flow. *Journal of Mechanical Science and Technology*. 28 (2014), 5, pp.1881-1885

26. Das K, Jana S, Kundu P.K., Thermophoretic MHD slip flow over a permeable surface with variable fluid properties, *Alexandria Engineering Journal*. 54 (2015), 1, pp. 35–44

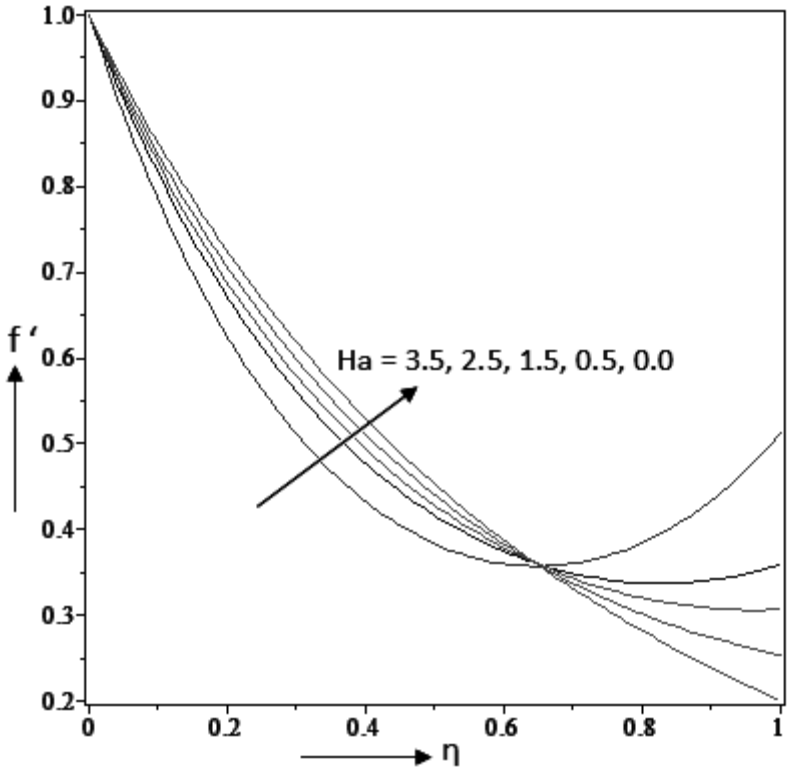

Figure 2. Velocity profiles for various values of Hartmann number Ha

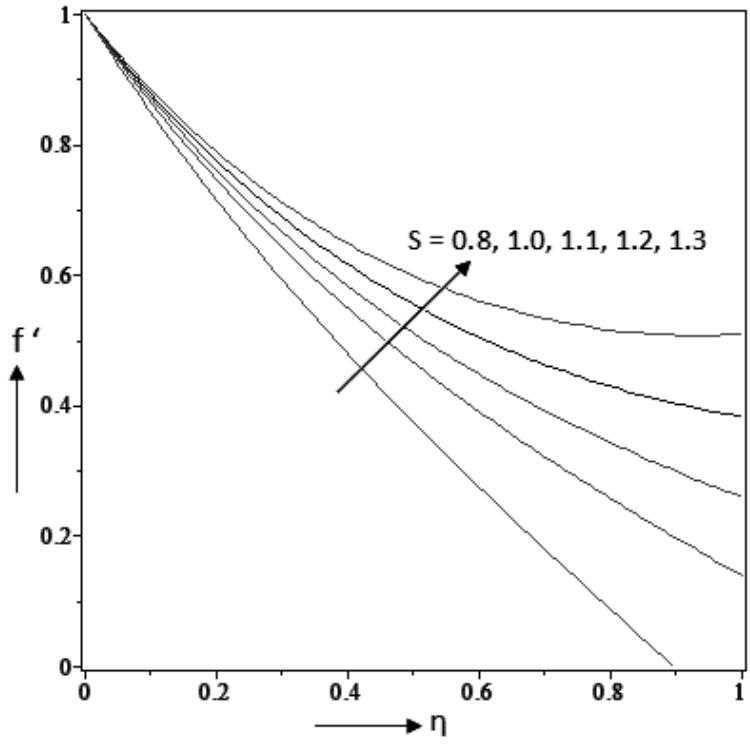

Figure 3. Velocity profiles for various values of unsteadiness parameter S

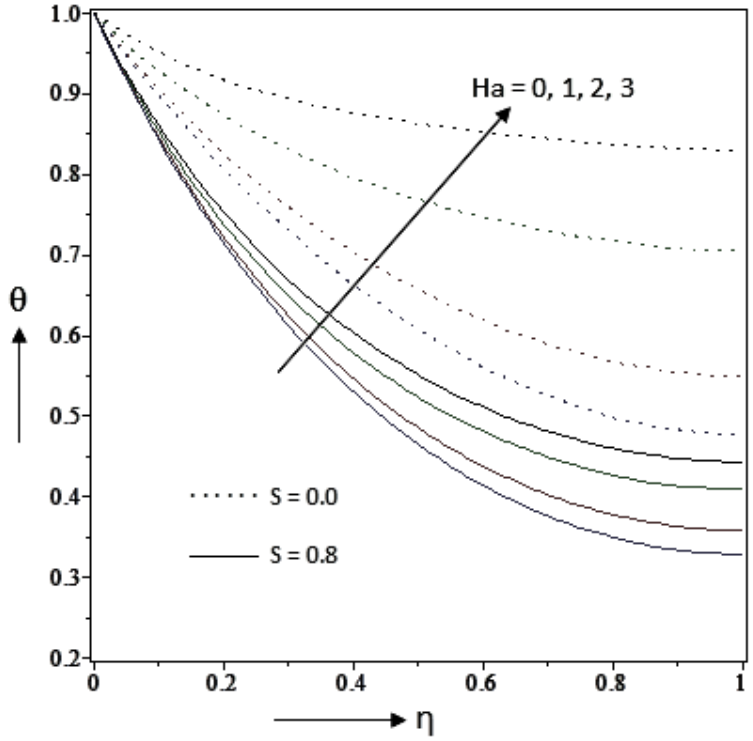

Figure 4. Temperature profiles for various values of Hartmann number Ha

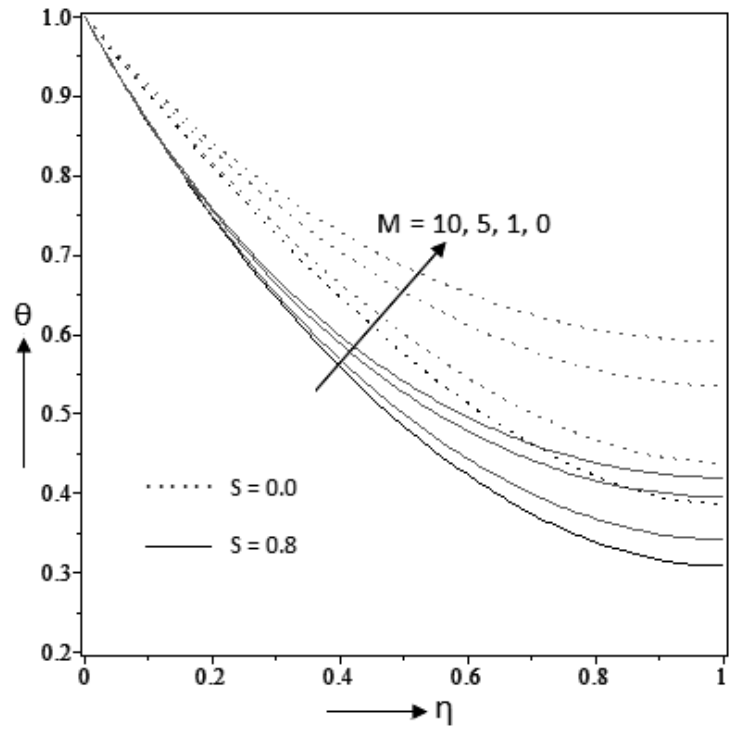

Figure 5. Temperature profiles for various values of thermocapillarity number M

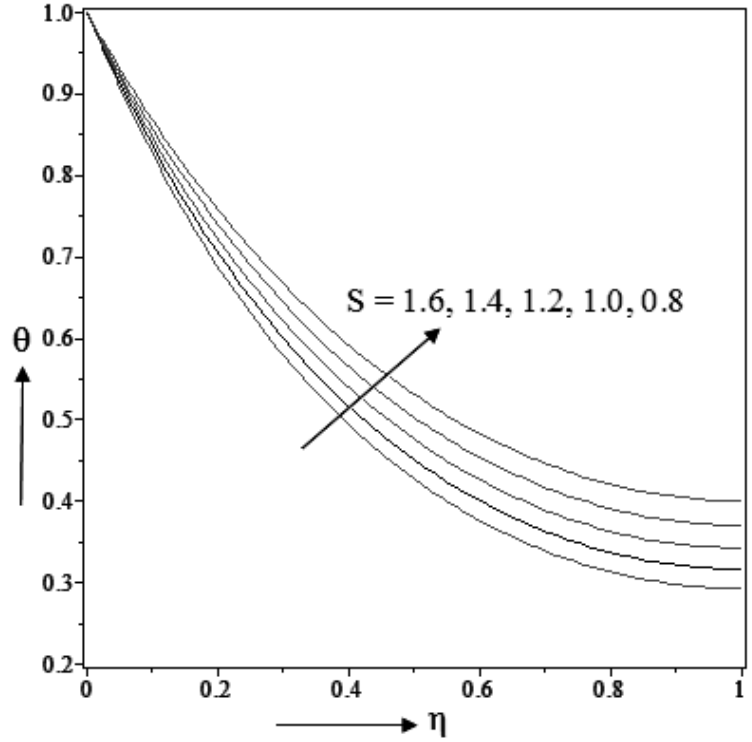

Figure 6. Temperature profiles for various values of unsteadiness parameter S

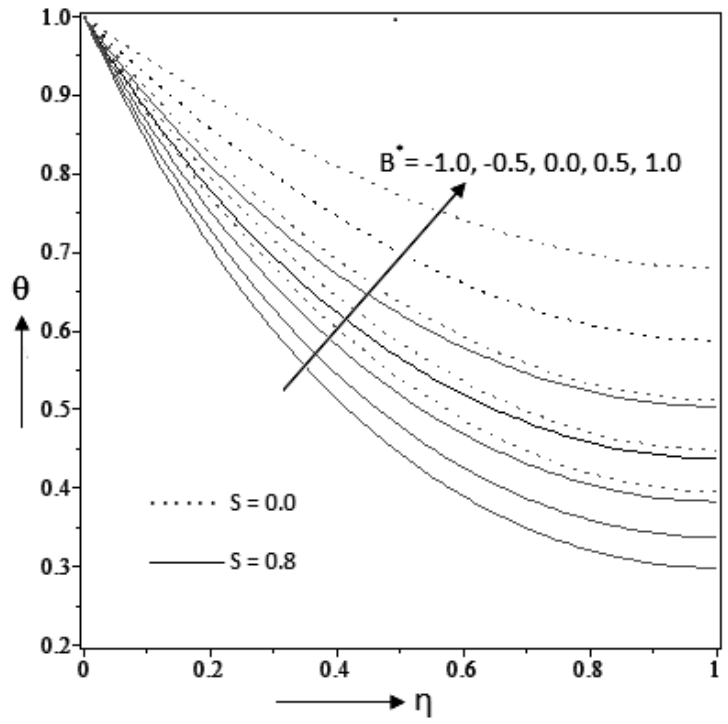

Figure 7. Temperature profiles for various values of heat generation/absorption parameter B^*

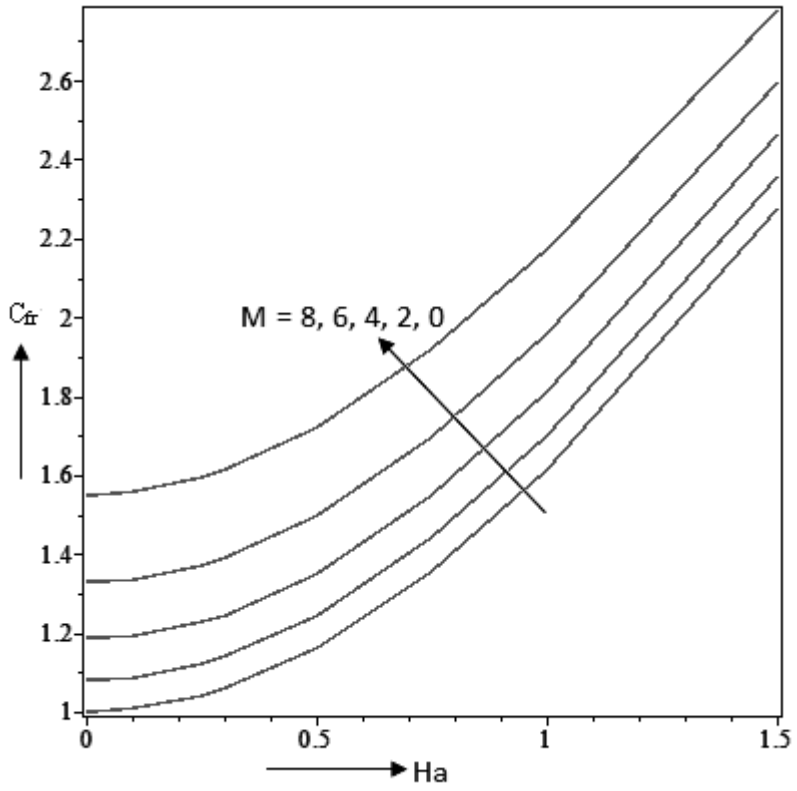

Figure 8. Variation of the reduced skin friction against Ha for various values of M

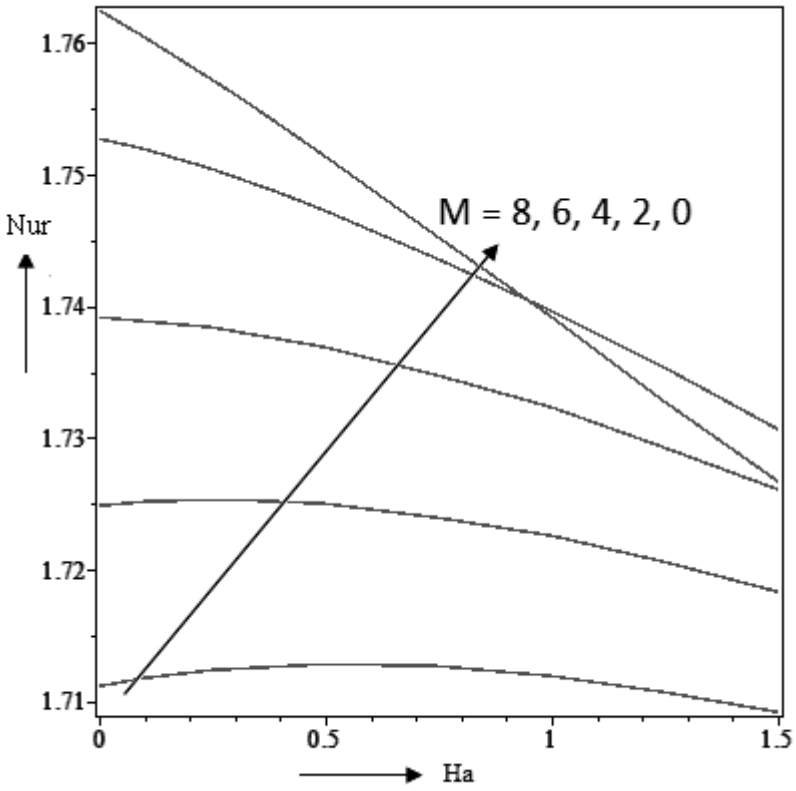

Figure 9. Variation of the reduced Nusselt number against Ha for various values of M

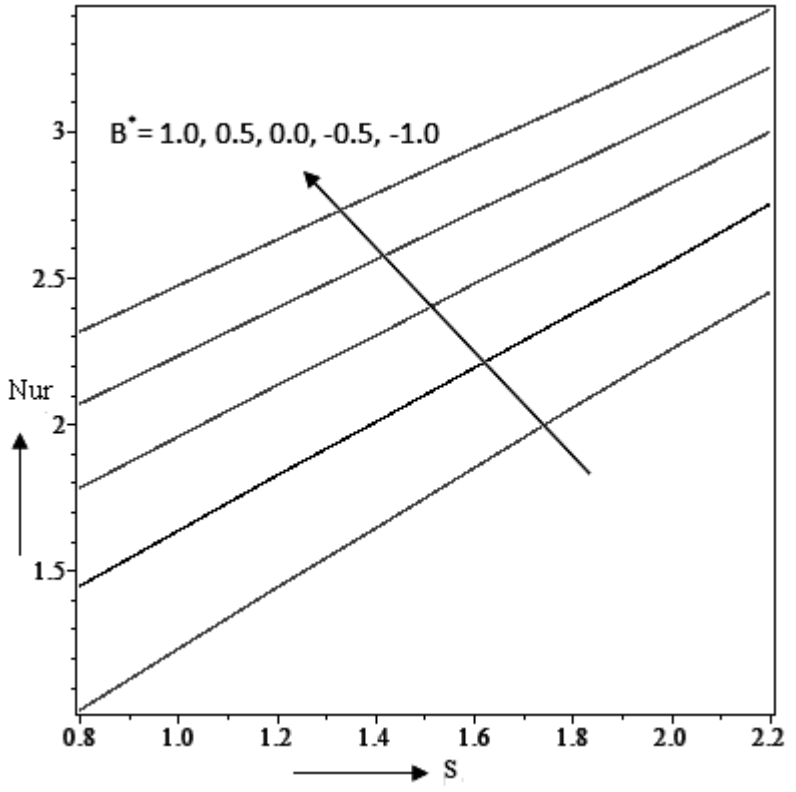

Figure 10. Variation of the reduced Nusselt number against S for various values of B*